

# Wide-Angle X-Band Antenna Array with Novel Radiating Elements

Roman CHERNOBROVKIN<sup>1</sup>, Igor IVANCHENKO<sup>1</sup>, Leo P. LIGTHART<sup>2</sup>,  
Aleksy KOROLEV<sup>3</sup>, Nina POPENKO<sup>1</sup>

<sup>1</sup> Usikov Inst. for Radiophys. and Electronics, National Acad. of Sciences, 12 Ac. Proskura St., Kharkov, 61085, Ukraine,

<sup>2</sup>Int. Research Centre for Telecommunications and Radar, Faculty of Electrical Engg., Mathematics and Computer Science, Delft University of Technology, Mekelweg 4, 2628 GA Delft, the Netherlands

<sup>3</sup>Inst. of Radioastronomy, National Academy of Sciences of Ukraine, 4 Krasnoznamenynaya st., 61085, Kharkov, Ukraine

ireburan@yahoo.com

**Abstract.** An antenna array with wide-angle beam steering is presented in this paper. The antenna consists of dielectrically filled open-ended waveguides with a new type of excitation as individual radiators. The characteristics of the radiator have been analyzed. The novel radiator has a wide beamwidth and the frequency band of around 21%. Following the computational modeling and experimental investigations the characteristics of the antenna array for scan angles up to  $50^\circ$  are discussed.

## Keywords

Antenna array, open-ended waveguide, near-field measurements, radiation pattern.

## 1. Introduction

The current progress in advanced communication systems leads to a particular interest in broadband phased array antennas with large scan angles [1-4]. It is worth noting, that there are challenging aspects to be solved in antenna arrays such as side lobe level decrease, as well as reduction of both antenna size and costs.

The following requirements imposed to the individual radiators of the antenna array should be satisfied:

1. The element bandwidth should be more than 20%;
2. The antenna array should ensure scan angles over more than  $45^\circ$  in both principal planes;
3. The polarization should be linear.

The structure of the antenna element consists of an open-ended waveguide with dielectric insertion comprising a special pin for excitation. The paper focuses on modeling of the individual radiator and the antenna array allowing for scan angles up to  $50^\circ$ , as well as the experimental investigations of the individual radiator and antenna array prototype.

## 2. Modeling of the Antenna Array

The antenna array characteristics are investigated in the frequency range 8 - 11GHz. The computational modeling was performed by using the software package HFSS. The radiation pattern measurements were carried out by the technique developed earlier [5] and allowed us to analyze quickly the radiation characteristics of the antenna under testing over the entire operational frequency band. The near-field distributions were measured by the probe described in [6].

### 2.1 The individual Element of the Antenna Array

The open-ended waveguide filled with a dielectric was chosen as individual radiator to provide an element spacing in the antenna array less than half a wavelength at 10 GHz. One of the novelties of the individual radiator is the transition from SMA to waveguide using an original excitation pin (Fig. 1).

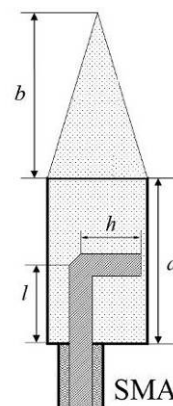


Fig. 1. Design of the individual radiator.

At first, we examined the parameter  $S_{11}$  of the semi-infinite rectangular waveguide filled with a dielectric ( $\epsilon=2.5$ ) and aperture dimensions  $14\text{mm}\times 7\text{mm}$ . The waveguide excitation is realized by means of a long coaxial transmission

line terminated with the pin (Fig. 1). The fundamental  $H_{10}$  mode propagates in the rectangular waveguide. In this case the pin dimensions equal length  $l=4\text{mm}$  and height  $h=5\text{mm}$ .

Field maps in Fig. 2 demonstrate the wave process in such a system and the electromagnetic field distribution close to the excitation pin.

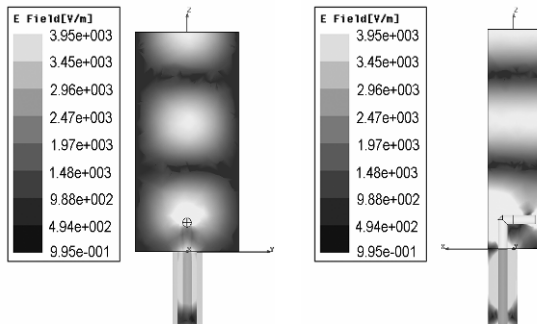


Fig. 2. Field maps for the semi-infinite waveguide excited by the coaxial transmission line.

In the frame of this research we analyzed the parameter  $S_{11}$  as function of the following parameters: pin height  $h$ , pin length  $l$ , length  $a$  of the waveguide regular part and height  $b$  of the dielectric prism. These parameters have been changed within the limits:  $2\text{ mm} < h < 4.5\text{ mm}$ ,  $2\text{ mm} < l < 13\text{ mm}$ ,  $5\text{ mm} < a < 15\text{ mm}$ ,  $0\text{ mm} < b < 30\text{ mm}$ . According to the results of computational modeling the individual radiator with parameters  $h = 4.5\text{ mm}$ ,  $l = 2.5\text{ mm}$ ,  $a = 5\text{ mm}$ ,  $b = 20\text{ mm}$  was chosen as basic element in the antenna array. Such radiator exhibits for  $S_{11} < -10\text{ dB}$  a bandwidth  $8.3\text{ GHz} < f < 13.0\text{ GHz}$  with the centre frequency around  $9\text{ GHz}$  (see Fig. 3, the theoretical curve).

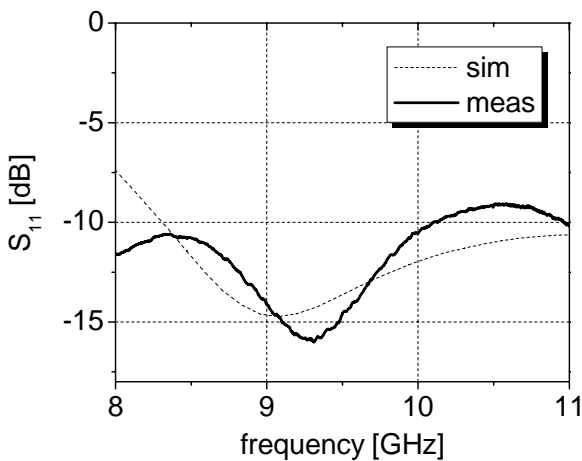


Fig. 3. Input reflection coefficient of the individual radiator excited by a coaxial feeding line.

For the individual radiator with the given parameters the radiation patterns in both principal planes have been calculated. As can be seen from Fig. 4, the radiation pattern of the individual radiator has a wide beamwidth in both H-plane ( $\Delta\theta=86^\circ$ ) and E-plane ( $\Delta\theta=96^\circ$ ) with a peak directivity oriented around zenith.

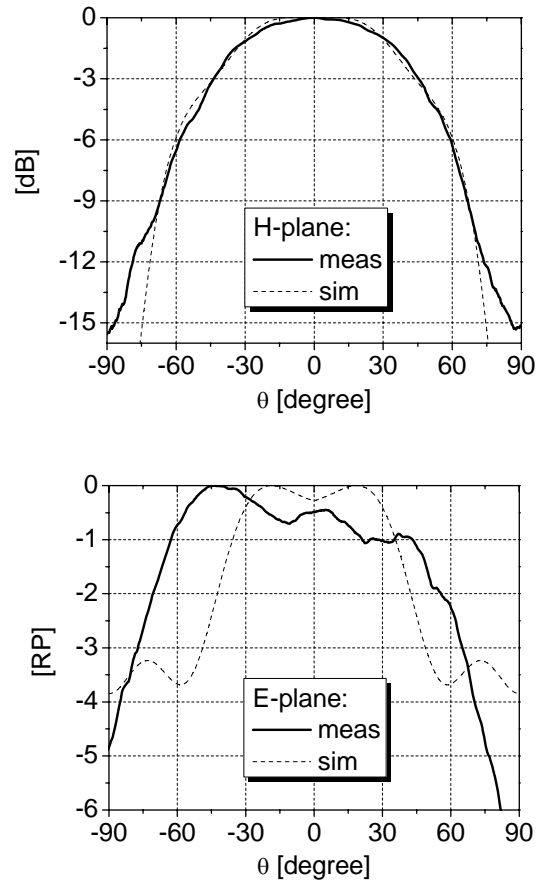


Fig. 4. Calculated and measured radiation patterns of the radiator prototype at  $9\text{ GHz}$  in the H-plane (top) and E-plane (bottom).

Following the results of computational modeling the individual radiator with the selected parameters was manufactured (Fig. 5) and its characteristics were investigated experimentally. We note that the measured and simulated input reflection coefficients are in good agreement. However, the experimental bandwidth of the radiator is less than the theoretical one ( $\Delta f=21\%$  in the experiment,  $\Delta f=30\%$  in the theory, see Fig. 3).

The pattern experiments have shown that the beamwidth of the radiator in the H-plane remains virtually the same over the operational frequency band (see Fig. 4). In contrast to the theory amplitude ripples of around  $1\text{ dB}$  are observed in the experimental radiation patterns in the E-plane. Furthermore, the measured beamwidth is broader ( $\Delta\theta=130^\circ$  in experiment and  $\Delta\theta=96^\circ$  in theory).

The main advantages of the novel individual radiator can be summarized as follows:

- A wide operational frequency band;
- A wide beamwidth in both principal planes over the entire operational frequency band;
- The original excitation pin allows for designing a compact antenna array with element spacing less than half of the smallest wavelength.

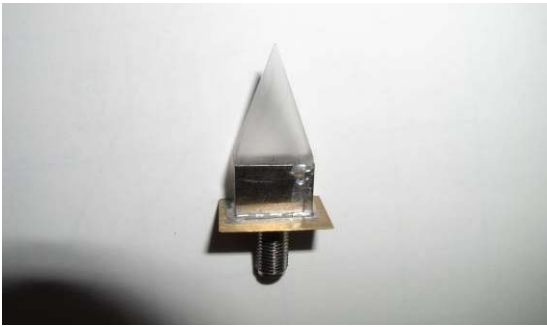


Fig. 5. Realized individual radiator.

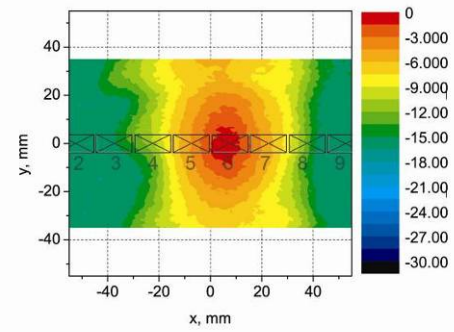
## 2.2 The Antenna Array

Based on our results of theoretical and experimental investigations we manufactured the linear array prototype, depicted in Fig. 6. The antenna array consists of 10 radiators with the same characteristics as mentioned earlier. The array elements are located in the H-plane at a mutual distance of 15mm. The minimum spacing between two adjacent radiators is therefore bounded by the thickness of the metallic walls associated to the waveguides. The aggregate length of the antenna amounts 30mm (SMA connector excluded).

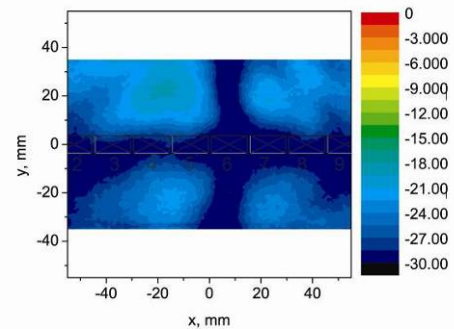


Fig. 6. Linear array prototype.

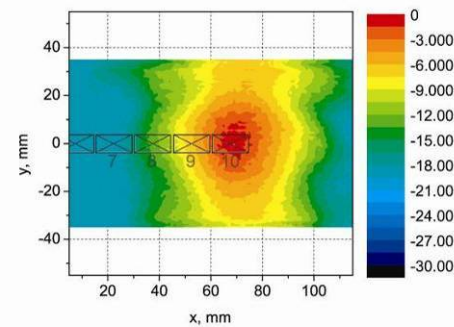
We have measured and analyzed the EM field distributions in the radiating region of each elementary radiator integrated in the antenna array. Co- and cross-polarizations per element have been investigated by having all other radiators terminated with matched loads. As an example, the near-field distributions of radiators 6 and 10 are shown in Fig. 7. It was found that the (co-polarization) near-field distribution in the XOY plane of each radiator is widened along the OY axis (Fig.7a, Fig.7c) due to the finite ground plane (width of the ground plane in the OY direction is 70 mm). It can also be seen that when exciting the central element 6 the field intensity decreases slowly to -13 dB at the antenna ends (Fig. 7a). From this study we have also learned that for the edge element 10 the maximal level of cross-polarization is higher (-13 dB) than that of the central element 6 (-18 dB). However, the shape of the near-field remains virtually the same in both cases (Fig. 7b and Fig. 7d).



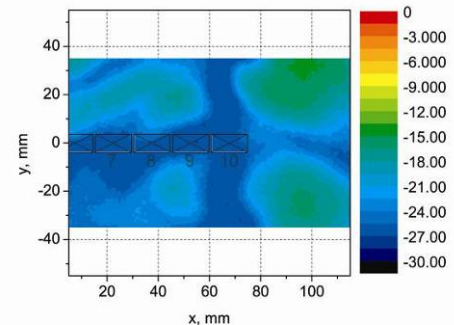
a



b



c



d

Fig. 7. Near-field distributions of two elements '6' and '10' within the array configuration in the XOY plane at 8.45 GHz; element 6: a - co-polarization, b - cross-polarization, element 10: c - co-polarization, d - cross-polarization.

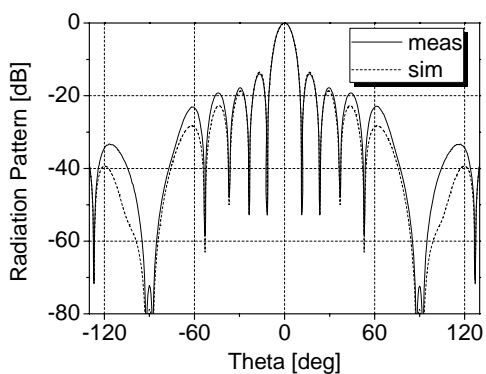
Calculated radiation patterns of the antenna array for different scanning angles were determined as follows. First, the array factor of the linear array prototype was simulated under the assumption of absence of mutual coupling between antenna array elements. After that, the calculated radiation patterns of the individual radiator (Fig. 4, simulated) were accumulated taking into account the path-length difference from different parts of the antenna array. As a result we obtained a set of radiation patterns for different scanning angles as given in Fig. 8 (sim.). More specifically, we derived from Fig. 8 that:

- the antenna exhibits a beamwidth of  $\Delta\theta=10^\circ$  (at -3 dB from the maximum);
- with increasing scanning angle the beamwidth slightly increases, too (Tab. 1).
- the side lobes are -17 dB for scanning angle  $\theta=0^\circ$  and a maximum side lobe level is observed for scanning angle  $\theta=50^\circ$ .

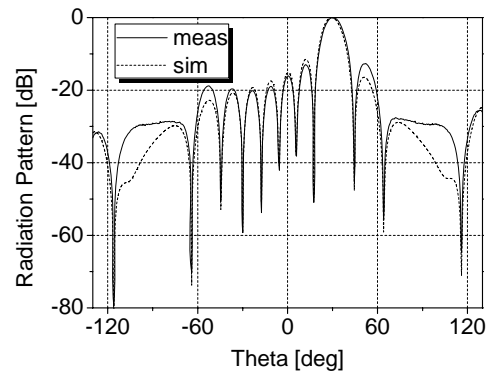
Scanning angle $\theta$	Calculation		Measurement	
	$\Delta\theta$	Side lobe level	$\Delta\theta$	Side lobe level
$0^\circ$	$10^\circ$	-17dB	$10^\circ$	-17dB
$30^\circ$	$12^\circ$	-11dB	$12^\circ$	-13dB
$50^\circ$	$14^\circ$	-9dB	$14^\circ$	-14dB

Tab. 1. Radiation pattern parameters of the antenna array.

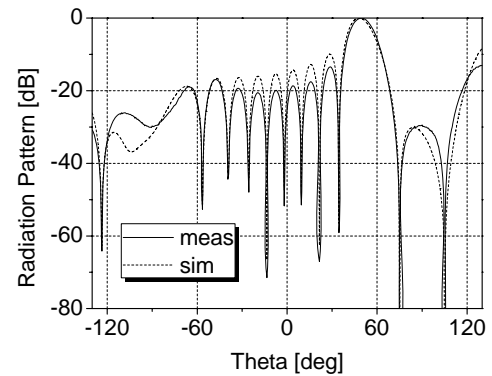
The radiation patterns of elementary radiators in the array configuration were measured in the H-plane at 8.45 GHz and having all other radiators terminated with 50  $\Omega$  matched loads (Fig. 9). In this case the radiation patterns (Fig. 8) of the antenna array calculated from measured and simulated data have the same beamwidths for all scanning angles (Tab. 1). A minimum side lobe level is observed for scanning angle  $\theta = 0^\circ$  (-17 dB) and it increases up to -9 dB for maximum scanning angle. From comparison of measured with simulated results it is noted that the level of side lobes for scanning angle  $\theta = 0^\circ$  is the same for the first two side lobes and the level of residual side lobes is higher. At the same time for other scanning angles the calculated radiation patterns have side lobe levels of the first four side lobes ( $\theta = 30^\circ$ ) and the first six side lobes ( $\theta = 50^\circ$ ) which are higher than in the antenna prototype (see Fig. 8).



a

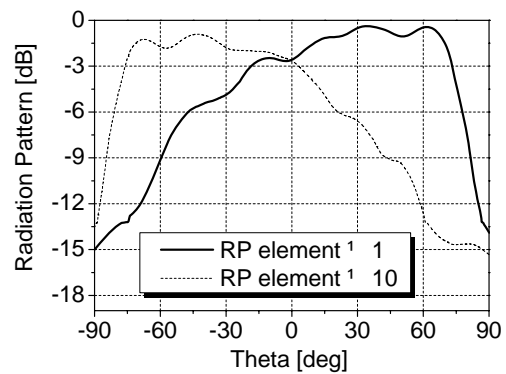


b

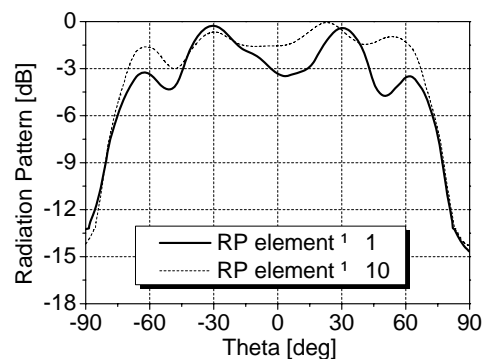


c

Fig. 8. Radiation patterns of the antenna array in the H-plane for different scanning angles: (a) scanning angle  $0^\circ$ ; (b) scanning angle  $30^\circ$ ; (c) scanning angle  $50^\circ$ .



a



b

Fig. 9. Radiation patterns of the elements 1 and 10 (a) and 5 and 6 (b) in the H-plane at 8.45 GHz.

As can be seen, the calculated and measured results demonstrate that the antenna array is able to provide beam steering in the limits of  $\pm 50^\circ$ .

### 3. Conclusions

A new type of individual radiator consisting of a dielectric filled waveguide antenna with special excitation pin has been proposed. The commercial Ansoft HFSS finite element based code has been used for radiator parameters optimization. As a result, the radiator prototype with an optimized geometrical configuration has been manufactured. The numerical simulations were validated by comparison with measurements performed on the physical model. The basic characteristics of the radiator prototype are as follows: (i) the beamwidth in the H-plane is  $\Delta\theta=100^\circ$  and in the E-plane is  $\Delta\theta=130^\circ$ ; (ii) the cross-polarization level is less than -15 dB over the entire operational frequency band.

The linear antenna prototype consisting of 10 individual radiators deployed in a uniform array configuration has been manufactured. The measurements of EM field distributions of individual elements of the array have been carried out in the radiating and far-field regions.

In agreement with the simulations, the scanning angle of the planar antenna array consisting of 10 elements is around  $\pm 50^\circ$  in H-plane and the side lobes level does not exceed -9 dB.

### Acknowledgements

This particular research was performed in the frame of the STCU Project P#217 titled "Theory and design of antenna arrays", and supported by the International Research Center for Telecommunications and Radar, Delft University of Technology, Netherlands. The responsibility for this publication is held by the authors only.

### References

- [1] HOLTER, H. Dual-polarized array antenna with BOR-elements, mechanical design and measurements. *IEEE Transactions on Antennas and Propagation*, 2007, vol. 55, no. 2, p. 305–312.
- [2] LEE, J. J., LIVINGSTONE, S., KOENING, R., NAGATA, D., LAI, L. L. Compact light weight UHF arrays using long slot apertures. *IEEE Transactions on Antennas and Propagation*, 2006, vol. 54, no. 7, p. 2009–2015.
- [3] THORS, B., STEYSKAL, H., HOLTER, H. Broadband fragmented aperture phased array element optimization using genetic algorithm. *IEEE Transactions on Antennas and Propagation*, 2005, vol. 53, no. 10, p. 3280–3287.
- [4] MCGRATH, D. T., BAUM, C. B. Numerical analysis of planar bicone and TEM horn antennas. *IEEE International Antennas and Propagation Symposium Digest*, June 1997, vol. 35, p. 1058–1161.
- [5] ANDRENKO, A. S., IVANCHENKO, I. V., IVANCHENKO, D. I., KARELIN, S. Y., KOROLEV, A. M., LAZ'KO, E. P., POPENKO, N. A. Active broad X-band circular patch antenna. *IEEE Antennas and Wireless Propagation Letters*, 2006, vol. 5, p. 529–533.
- [6] CHERNOBROVKIN R., IVANCHENKO I., POPENKO N. Novel V-band antenna for nondestructive testing techniques. *Microwave and Optical Technology Letters*, July 2007, vol. 49, no. 7, p 1732 to 1735.

### About Authors...

**Roman CHERNOBROVKIN** was born in Kharkov, Ukraine, in 1983. In June 2005 he graduated from the Kharkov National University and received the MS degree in Radio Physics. From 2005 to the present he works at the Institute for Radio-Physics & Electronics of the National Academy of Sciences of Ukraine (IRE NASU). From 2007 he is a Junior Researcher Assistant with the Department of Radio-Spectroscopy in the IRE NASU. He has authored and co-authored 8 publications in the fields of micro - and millimeter wave antennas. R. Chernobrovkin is the Student Member of IEEE.

**Igor IVANCHENKO** – for biography, see page 65 of this issue.

**Leo P. LIGTHART** was born in Rotterdam, the Netherlands, on September 15, 1946. He received an Engineer's degree (cum laude) and a Doctor of Technology degree from Delft University of Technology in 1969 and 1985, respectively. He is fellow of IEE and IEEE. He received Doctorates (honoris causa) at Moscow State Technical University of Civil Aviation in 1999 and Tomsk State University of Control Systems and Radioelectronics in 2001. He is academician of the Russian Academy of Transport.

Since 1992, he has held the chair of Microwave Transmission, Radar and Remote Sensing in the Department of Electrical Engineering, Mathematics and Computer Science, Delft University of Technology. In 1994, he founded the International Research Center for Telecommunications and Radar (IRCTR) and is the director of IRCTR. Prof. Ligthart's principal areas of specialization include antennas and propagation, radar and remote sensing, but he has also been active in satellite, mobile and radio communications. He has published over 500 papers and 2 books.

**Alexey KOROLEV** and **Nina POPENKO** – for biographies, see page 65 of this issue.